PCCP

RSC Publishing

PAPER

Mitigation of CO poisoning on functionalized Pt–TiN surfaces†

Cite this: *Phys. Chem. Chem. Phys.*, 2013, **15**, 19450

R. Q. Zhang,[ab] C.-E. Kim,[a] B.-D. Yu,[c] C. Stampfl[da] and A. Soon*[ad]

Received 6th August 2013,
Accepted 1st October 2013

DOI: 10.1039/c3cp53334d

www.rsc.org/pccp

It has been previously reported that the system of single Pt atoms embedded in N-vacancy (V_N) sites on the TiN(100) surface (Pt–TiN) could be a promising catalyst for proton exchange membrane fuel cells (PEM FCs). The adsorption of molecules on Pt–TiN is an important step, when it is incorporated as the anode or cathode of PEM FCs. Utilizing first principles calculations based on density functional theory, systematic investigations are performed on the adsorption of several atomic and molecular species on the Pt–TiN system, as well as the co-adsorption of them. The favorable binding sites and adsorption energies of several molecular species, namely carbon dioxide (CO_2), carbon monoxide (CO), oxygen (O_2), hydrogen (H_2), hydroxyl (OH), an oxygen atom (O), and a hydrogen atom (H), are explored. For each, the adsorption energy and preferred binding site are identified and the vibrational frequencies calculated. It is found that CO_2, CO and H prefer the Pt top site while OH and O favorably adsorb on the Ti top site. When CO and OH are co-adsorbed on the Pt–TiN(100) surface, OH weakens the adsorption of CO. The weakening effect is enhanced by increasing the coverage of OH. A similar behavior occurs for H and OH co-adsorption on the Pt–TiN(100) surface. Because co-adsorption with OH and H species weakens the adsorption of CO on Pt–TiN, it is expected that the acid and base conditions in PEM FCs could mitigate CO poisoning on functionalized Pt–TiN surfaces.

Introduction

Heterogeneous catalysis has received a tremendous amount of interest, both from a scientific and industrial perspective. Due to the enormous scale of commercial applications, progress in catalysis can have a positive economic as well as environmental impact, particularly in the area of clean energy technologies. More specifically, the automotive and power generation (*e.g.* fuel cells) industries are the sectors that stand to benefit most directly from breakthroughs that are expected to occur in the field of catalysis. Amongst the various types of fuel cells studied thus far, proton exchange membrane fuel cells (PEM FCs) have received broad attention due to their low operating temperature, low weight, low emissions and quick start-up time.[1,2] Two major drawbacks for the efficient use of PEM FCs are namely their high production costs (due to the use of the Pt catalyst) and their low material durability (resulting in poor cycle life).[3] In order to increase the efficiency per Pt atom and enhance the durability, our previous work demonstrated that the system of a single Pt atom embedded in the V_N site on the TiN(100) surface (Pt–TiN) could be a promising candidate for a catalyst in PEM FCs.[4] The use of a single Pt atom decreases high production costs, and the high resistance to corrosion of TiN ensures high material durability in PEM FCs. Recent studies have found that TiN nanoparticles showed a relatively high performance for PEM FC reactions (especially under alkaline conditions),[5] while another report claims that the catalyst of a single-atom Pt anchored to graphene exhibited significantly improved catalytic activity (up to 10 times) over that of the state-of-the-art commercial Pt/C catalyst.[6]

Adsorption of atomic or molecular species on surfaces modifies the electronic and structural properties, thus affecting their catalytic properties. The interaction between adsorbates such as atoms, molecules, and ions on catalyst surfaces is key to understanding catalyzed reactions. A detailed knowledge of the adsorption properties of the Pt–TiN system is necessary before undertaking further study of its catalytic properties. Carbon dioxide (CO_2) and carbon monoxide (CO) are the contaminants in the reactions of PEM FCs. Oxygen (O_2) and hydrogen (H_2) are reactants for the cathodic and anodic reactions, respectively. In addition, the adsorption of hydroxyl (OH), oxygen atoms (O), and hydrogen atoms (H) determines the activation energies of

[a] *Global E[3] Institute and Department of Materials Science and Engineering, Yonsei University, 120-749, Seoul, Korea. E-mail: aloysius.soon@yonsei.ac.kr*
[b] *School of Chemical Engineering and Bioengineering, Washington State University, 99163, WA, USA*
[c] *Department of Physics, University of Seoul, Seoul 130-743, Korea*
[d] *School of Physics, The University of Sydney, Sydney, NSW 2006, Australia*

† Electronic supplementary information (ESI) available. See DOI: 10.1039/c3cp53334d

the reactions. Thus, we systematically investigate the adsorption behaviors of these atomic and molecular species on the Pt–TiN system.

Carbon monoxide (CO) poisoning of catalysts is one of the important challenges that hinder the large-scale commercialization of proton exchange membrane fuel cells. In addition, the effect of CO_2 contamination on the anode catalyst is similar to that of CO. Carbon dioxide is reduced to CO, which strongly adsorbs on Pt, blocking H_2 adsorption. There have been many studies aimed at resolving this CO poisoning issue.[7–10] Effects of electron and hole doping in Pt_4 clusters suggested an effective method to prevent the CO poisoning through regulating the total charge in Pt_4 clusters.[7] It is reported that intermetallic compounds show superior catalytic properties. CO on the $PtBi_2$ and PtBi surfaces presents much lower adsorption energies than on metallic Pt by raising the Fermi level of the $PtBi_2$ and PtBi surfaces. Then it decreases CO poisoning effects on $PtBi_2$ and PtBi electrodes.[8] Kapur *et al.* demonstrated that Bi-modified Pt(111) surfaces reduced CO poisoning because Bi dopants prohibit CO adsorption.[9] Bimetallic Pt–Ti nanoalloys exhibit enhanced properties compared to pure Pt catalysts, because of the weaker binding of CO on these alloys compared to pure Pt clusters.[10]

Recently, it has been demonstrated that CO doesn't desorb on an Au(111) surface in aqueous alkaline media. However, on this CO-modified Au(111) surface, CO can act as a promoter for the electrocatalytic oxidation of certain alcohols, in particular methanol.[11] This is an excellent example of the promotion effect by co-adsorbed molecules in electrocatalysis. There are many studies concerning the adsorption enhancement of CO on the Au(111) surface by co-adsorbed Cl,[12] NO_2,[13] sulfate ions,[14] S,[15] and OH.[16] This phenomenon is induced by electron transfer from CO to the other molecules. The more electrons transferred to the substrate from CO, the greater the adsorption energy of CO. Meanwhile, Na-induced surface negative charging weakens CO adsorption on Au(111) surfaces[15] and NO adsorption on the Pd(111) surface.[17] Carbon monoxide adsorbed on the Au(111) surface significantly decreases the onset potential for methanol oxidation.[11] The mechanism of this promotion effect is that the presence of adsorbed CO promotes beta-hydrogen elimination, that is, C–H bond breaking. The adsorption of OH, induced by CO on Au(111), catalyses a very specific step in the oxidation of the alcohol. It is found that the enhancement of CO adsorption by S on Au originates from a S-induced positive polarization of the Au surface.[15]

For the system of Pt particles deposited on TiN surfaces, it is revealed experimentally that the surface Ti–OH type functional groups help in reducing the accumulation of CO on the catalyst surface when OH and CO molecules co-exist.[18] It was found that the electron deficiency on Pt may enhance accumulation of hydroxyl groups on its surface which would help in the removal of adsorbed CO on Pt.[18] However, for the Pt–TiN system, the Pt atom presents a negative charge, where a "ring" of negative charge about the Pt atom appears.[4] Thus, it is necessary to investigate the co-adsorption of CO and OH on the Pt–TiN system, as well as the co-adsorption of CO and H.

Based on the above description, in the present paper, by performing first-principles calculations based on density functional theory (DFT), the adsorption behaviors of different atomic and molecular species on the Pt–TiN(100) surface are investigated. It is found that the adsorption energy of CO on Pt–TiN is lower than that for CO on the Pt(111) surface. Therefore, Pt–TiN appears to be more efficient than the Pt(111) surface in relation to reducing the effect of CO poisoning. It is found that, on Pt–TiN surfaces, OH (or H) decreases the adsorption energy of CO and hence reduces the accumulation of CO. These results imply that the CO poisoning may not occur for Pt–TiN in the alkaline (or acidic) environment.

Computational method

We use the Vienna *ab initio* Simulations Package (VASP 5.2) code.[19–21] We employ the projector-augmented-wave (PAW) method and the generalized-gradient approximation (GGA) due to Perdew, Burke and Ernzerhof (PBE)[22] for the exchange–correlation functional. For electron–ion interactions, the projector-augmented-wave (PAW) method was used.[21] The electronic wave functions are expanded in a plane wave basis set with a kinetic-energy cutoff of 500 eV. From our previous study of pristine TiN and its crystal morphology, it is shown that the predominant facet exposed is the (100) surface and thus we have chosen this facet to study the Pt–TiN system.[23] The Pt–TiN system consists of a Pt atom adsorbed on a V_N site of a TiN(100) $p(3 \times 3)$ surface cell. Details concerning the atomic structures can be found in our previous work.[4] We consider molecular adsorption in different sites on the surface. Fig. 1(a) shows the adsorption sites considered, namely the Pt top site (T_{Pt}), the Ti top site (T_{Ti}), and the Ti bridge site (B_{Ti}). The *k*-space integration is performed using a $4 \times 4 \times 1$ mesh in the Brillouin zone for the

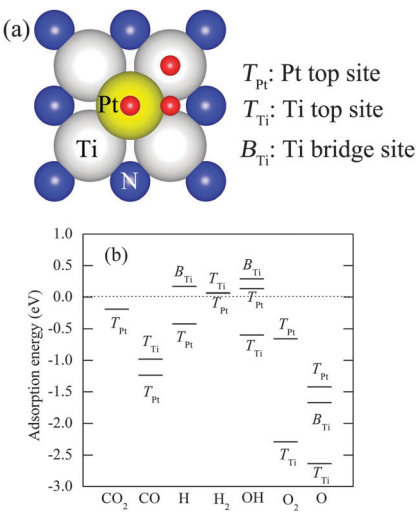

Fig. 1 (a) The adsorption sites considered (the smallest balls) on the surface of the Pt–TiN system. (b) The adsorption energy (with ZPE correction) for the different atoms and molecules adsorbed on the Pt–TiN(100) surface. The positive and negative values correspond to adsorption that is either endothermic or exothermic, respectively. The dotted line indicates the energy zero. The corresponding adsorption energy values are presented in Table S1 of ESI.†

$p(3 \times 3)$ surface cell. A Methfessel–Paxton smearing of 0.1 eV is used to improve the convergence and the total energy is extrapolated to zero temperature. Dipole corrections[24] of the electric potential and total energy are imposed to eliminate dipole–dipole interactions of images between supercells. The convergence criterion for the total energy is taken to be smaller than 1×10^{-5} eV, while for geometry optimization, the ionic relaxations are performed until the net change in the forces acting on the atoms becomes smaller than 1×10^{-2} eV Å^{-1}.

The adsorption energy E_{ad} with zero-point energy (ZPE) corrections, for different atoms and molecules adsorbed on the Pt–TiN(100) surface is defined as follows:

$$E_{ad} = E_{tot} - E_{TiN}^{Pt} - E_M + \Delta ZPE \quad (1)$$

where E_{tot} and E_{TiN}^{Pt} are the total energies of the adsorption system and Pt–TiN(100) system, respectively. M denotes the different atoms or molecules adsorbed on the surface. For O and H atoms, and the CO molecule, the adsorption energy is with respect to the O_2, H_2, and CO molecules, respectively. For the OH molecule, the adsorption energy is with respect to the H_2 and H_2O molecules. Thus, $E_O = \frac{1}{2}E_{O_2}^{mlc}$, $E_H = \frac{1}{2}E_{H_2}^{mlc}$, $E_{CO} = E_{CO}^{mlc}$, $E_{OH} = E_{H_2O}^{mlc} - \frac{1}{2}E_{H_2}^{mlc}$, where $E_{O_2}^{mlc}$, $E_{H_2}^{mlc}$, E_{CO}^{mlc}, and $E_{H_2O}^{mlc}$ are the total energies of the free molecules O_2, H_2, CO, and H_2O respectively. $\Delta ZPE = ZPE_{Pt-TiN}^{M} - ZPE_{Free}^{M}$, where ZPE_{Pt-TiN}^{M} and ZPE_{Free}^{M} are the ZPEs of molecules adsorbed on Pt–TiN(100) and the free molecules, respectively. The adsorption energy of Pt, E_{Pt}^{ad}, was also calculated when atoms and molecules are adsorbed. Here, the ZPE correction is also considered. The adsorption energy is defined by:

$$E_{Pt}^{ad} = E_{tot} - E_{TiN} - E_{bulk}^{Pt} - E_M + \mu_N + \Delta ZPE \quad (2)$$

where E_{TiN} is the total energy of the TiN slab with a surface N vacancy and E_{bulk}^{Pt} is the total energy of bulk Pt. μ_N is the atomic chemical potentials of N. Under N-lean conditions, $\mu_{Ti} = E_{Ti}^{bulk}$ and $\mu_N = E_{TiN}^{bulk} - \mu_{Ti}$, while under N-rich conditions, $\mu_N = \frac{1}{2}E_{N_2}^{mlc}$ and $\mu_{Ti} = E_{TiN}^{bulk} - \mu_N$, where E_{TiN}^{bulk}, E_{Ti}^{bulk} and $E_{N_2}^{mlc}$ are the total energies of bulk TiN, bulk Ti and the N_2 molecule, respectively.

For co-adsorption of CO with OH and H groups, the adsorption energy of CO, E_{CO}^{ad}, is defined as:

$$E_{CO}^{ad} = E_{tot} - E_{Pt-TiN}^{M} - E_{CO}^{mlc} \quad (3)$$

where E_{tot} and E_{Pt-TiN}^{M} are the total energies of the co-adsorption system and M (OH or H groups) adsorbed on the Pt–TiN system, respectively.

We define two kinds of the charge density difference distributions, $\Delta\rho_1$ and $\Delta\rho_2$, as follows:

$$\Delta\rho_1 = \rho^{sys} - \rho^{Pt-TiN} - \rho^{M} \quad (4)$$

$$\Delta\rho_2 = \rho^{sys} - \rho^{TiN} - \rho^{PtM} \quad (5)$$

where ρ^{sys}, ρ^{Pt-TiN}, ρ^{M}, ρ^{TiN}, and ρ^{PtM} are the charge densities of the adsorption system, the Pt–TiN slab system, M (O, H, CO, OH) molecules, the TiN slab, and Pt atoms with M molecules, respectively. In the calculation of the latter two quantities in the above equations, the atomic positions are fixed as those they have in the adsorption system. $\Delta\rho_1$ shows the electron transfer between molecules and the Pt–TiN slab, while $\Delta\rho_2$ shows electron transfer between Pt with molecules and the TiN substrate with a N vacancy.

Results and discussion

We firstly calculated the vibrational frequencies for the free molecules. The effect of spin polarization is taken into account. The vibrational frequencies (analyzed in bond bending and bond stretching modes) for each molecule are listed in Table 1. It is found that our results are in good agreement with experimental and theoretical results.

Fig. 1(b) displays the adsorption energy (with ZPE corrections) for the different atoms and molecules adsorbed on the Pt–TiN system. On the whole, CO_2, CO, and the H atom prefer the T_{Pt} site, while O_2, OH, and O prefer to adsorb on the T_{Ti} site. The values are listed in Table 2. For CO_2 adsorption, when it is initially placed on the T_{Ti} site, CO_2 migrates to the T_{Pt} site without an energy barrier. In addition, on the T_{Pt} site, the bond angle of O–C–O of CO_2 is 147°, a significant difference to that of free CO_2 which is 180°. The low adsorption energy of −0.17 eV implies that CO_2 could not poison the Pt–TiN system. Here, a negative value indicates binding and a positive value indicates that adsorption is not stable. For CO adsorption, although the T_{Pt} site is the more favorable site, CO can also be metastable on the T_{Ti} site, with an adsorption energy of −0.98 eV. When the CO molecule was initially placed on the B_{Ti} site, it diffused to the T_{Pt} site. It is interesting to note that the adsorption energy of CO adsorbed on the Pt–TiN system, which is −1.24 eV, is

Table 1 Calculated vibrational frequencies for the various molecules. Available experimental values of the vibrational frequencies are taken from ref. 29. The unit is cm^{-1}. The bond bending and stretching modes are indicated by δ and ν, respectively

	Frequencies		
Molecule	This work	Exp.	Vibration mode
CO	2189	2170	ν_{CO}
O_2	1615	1580	ν_{OO}
CO_2	2357, 1316	2349, 1333	ν_{CO} and δ_{CO}
	632	667	
H_2	4325	4401	ν_{HH}
OH	3641	3738	ν_{OH}

Table 2 The most stable adsorption site for the different atomic and molecular species adsorbed on Pt–TiN. The corresponding adsorption energies of Pt under different conditions (N-lean and N-rich) are also listed

		E_{Pt}^{ad} (eV)	
Species	The most stable site	N-lean	N-rich
CO_2	T_{Pt}	−1.30	2.14
CO	T_{Pt}	−2.35	1.10
O_2	T_{Ti}	−3.41	0.04
H_2	T_{Pt}	−1.05	2.40
OH	T_{Ti}	−1.73	1.72
O	T_{Ti}	−3.75	−0.30
H	T_{Pt}	−1.54	1.91

higher (less favorable) than that of CO adsorbed on the Pt(111) surface (−1.68 eV).[25] This indicates that Pt–TiN may perform better than the Pt(111) surface with regard to CO poisoning. For the adsorption of the O_2 molecule and the O atom, both prefer the T_{Ti} site and bind strongly to the surface. As shown in Fig. 2(b), the adsorption energy of H_2 adsorbed on the Pt–TiN system is positive, *i.e.* unstable. The adsorption energy of OH is calculated with respect to H_2O and H_2 molecules, instead of the OH species. However, if the adsorption energy of OH is calculated with respect to the OH species, it is −2.87 eV, −3.02 eV, and −3.75 eV for the B_{Ti} site, T_{Pt} site, and T_{Ti} site, respectively. It is found that the T_{Pt} and B_{Ti} sites are unstable adsorption sites for OH, while the T_{Ti} site is a stable binding site for OH on the Pt–TiN system. In the T_{Ti} site, the H atom of OH tilts at an angle of 48.7° with respect to the surface plane. We also calculated the adsorption energy of Pt for molecules adsorbed on the Pt–TiN system (*cf.* eqn (2)) under N-lean and N-rich conditions. The results are listed in Table 2. It is found that the adsorbed molecules enhanced the adsorption energy of Pt, compared to the situation without molecular adsorption (see Table 2 in ref. 4). We also calculated the frequencies of the molecular species adsorbed on the Pt–TiN system, as shown in Table 3. The shift in frequency can be used as an experimental tool to probe the properties of adsorbed species. CO, H_2, and OH have blue shifts of 568 cm^{-1}, 542 cm^{-1}, and 1309 cm^{-1}, respectively, compared to the free molecules, while CO_2 and O_2 present a red shift in frequency.

Here, since our goal is to investigate the CO poisoning issue, we further discuss the properties of CO adsorption. For CO adsorption, the favorable site is the T_{Pt} site. The bond length of CO adsorbed in this site is 1.168 Å, representing an increase relative to that of the free CO molecule (1.144 Å). This change is induced by electron back donation from Pt. In addition, the vibrational frequency of CO adsorbed on the T_{Pt} site is 2757 cm^{-1}, a blue shift of 657 cm^{-1} with respect to the vibrational frequency of CO adsorbed on the Pt(111) surface (2100 cm^{-1}).[26]

In Fig. 2 the charge density differences of CO adsorbed on the T_{Pt} site of the Pt–TiN system is shown, as obtained from eqn (4) and (5). Fig. 2a displays the electron transfer between CO and Pt–TiN, while Fig. 2b presents the electron transfer between the complex of CO–Pt and the TiN surface. As can be seen from Fig. 2a, there is depletion of electron density on the Pt atom and accumulation of electron density around CO, that is, there is electron transfer from Pt to CO. For the electron redistribution between the complex of CO–Pt and the TiN surface, although it is similar to the Pt–TiN system before adsorption,[4] the electron transfer from Pt to CO enhances the adsorption energy of Pt, as shown in Table 2. Fig. 2c shows the partial electronic density-of-states (PDOS) of C, O, and Pt atoms for CO adsorbed on the Pt–TiN system, as well as the PDOS of a Pt atom in the Pt–TiN system without adsorbed CO. After CO adsorption, it can be seen that Pt 5d states present a shift to lower energies and a peak around −2.3 eV appears. These variations are due to the interaction between Pt 5d states and CO orbitals, *i.e.* the electron back-donation to the 2π* orbital of CO. In addition, the peak around −3.8 eV in the Pt 5d states and the CO 5σ orbital displays the interaction between them.

Fig. 3 shows the charge density differences and projected density of states (PDOS) for OH adsorbed on the T_{Ti} site in the Pt–TiN system. As shown in Fig. 3a, although OH is adsorbed on the T_{Ti} site, there is electron transfer between Pt and OH because of the close distance between the Pt and O atoms of 2.505 Å. The O atom gains electron density from the Pt and Ti atoms, which results in formation of an electron depletion area

Table 3 Calculated vibrational frequencies at the Γ point for molecules adsorbed on the Pt–TiN(100) surface. The unit is cm^{-1}. The corresponding values of the free molecules are shown for comparison

	Frequencies		
Molecule	Adsorbed	Free	Vibration mode
CO_2	1884, 1182 590	2357, 1316 632	ν_{CO} and δ_{CO}
CO	2757	2189	ν_{CO}
O_2	1470	1615	ν_{OO}
H_2	4867	4325	ν_{HH}
OH	4950	3641	ν_{OH}

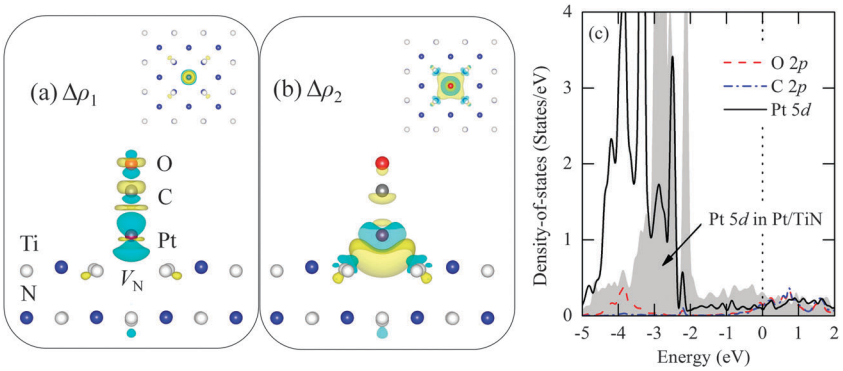

Fig. 2 Side view of electron charge density differences of (a) $\Delta\rho_1$ (*cf.* eqn (4)) and (b) $\Delta\rho_2$ (*cf.* eqn (5)) for CO adsorbed on the Pt–TiN system in the Pt site. The insets show the corresponding top-view. Charge accumulation and depletion are represented by the yellow and light blue regions, respectively. The isosurface levels are ±0.005 e $Bohr^{-3}$. (c) The partial density-of-states for CO adsorbed on the Pt–TiN system. The PDOS for Pt 5d states in Pt–TiN without CO represented by the shaded curved are given for comparison. The Fermi energy is indicated by the vertical dotted line at 0 eV.

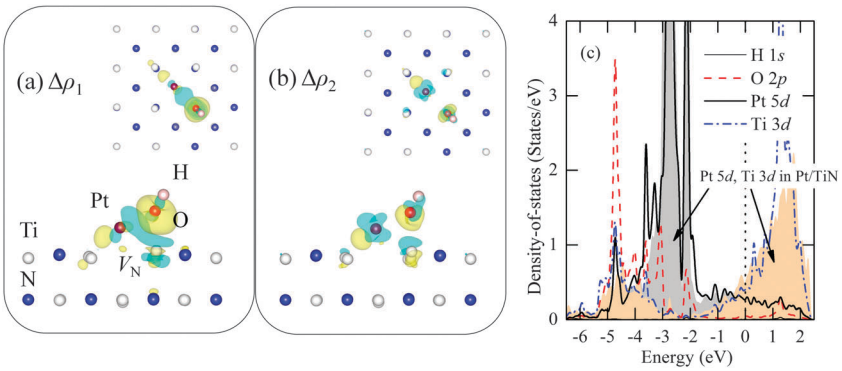

Fig. 3 Side view of electron charge density differences of (a) $\Delta\rho_1$ (*cf.* eqn (4)) and (b) $\Delta\rho_2$ (*cf.* eqn (5)) for OH adsorbed on the Pt–TiN system, where the inset shows the corresponding top-view. Charge accumulation and depletion are represented by the yellow and light blue regions, respectively. The isosurface levels are ±0.005 e Bohr^{-3}. (c) The partial density-of-states for OH adsorbed on the Pt–TiN system. The PDOS for Pt 5d states in Pt–TiN without OH represented by the shaded curved are given for comparison. The Fermi energy is indicated by the vertical dotted line at 0 eV.

around the Pt and Ti atoms. This is confirmed by the PDOS, as shown in Fig. 3c. It can be seen that there is an interaction between the Pt 5d states, Ti 3d states and O 2p states where the two peaks at −4.7 eV and −3.8 eV appear. From the top view of $\Delta\rho_1$ (Fig. 3c), the charge redistribution is directional and both Pt and Ti atoms are involved in the charge transfer. For the electron transfer between the Pt–OH complex and TiN substrate, as shown in Fig. 3b, it is demonstrated again that the charge redistribution occurs among Pt, O, and Ti atoms. Because of the loss of electrons from the Ti atom, there are more Ti 3d conduction states than that of the Ti atom in the Pt–TiN system without adsorption, as displayed in Fig. 3c. Note that the d-band center of Pt exhibits a decrease of 0.14 eV after OH adsorption on the T_{Ti} site. It is expected that this small variation of the d-band center will not affect the catalytic properties of the Pt site significantly.

For H atom adsorption, it is stable on the T_{Pt} site with an adsorption energy of −0.43 eV. This is significantly smaller than that on the Pt(111) surface of −2.7 eV.[6] Note that when H is adsorbed on the B_{Ti} site, it is unstable with the positive adsorption energy of 0.13 eV. For H adsorbed on the T_{Pt} site in the Pt–TiN system, Fig. 4 shows the charge density differences and the PDOS. It can be seen that H atom gains electron density from the Pt atom, as shown in Fig. 4a. Combined with the PDOS shown in Fig. 4c, it is found that a H1s–Pt5d$_{zz}$ hybrid orbital is formed between the H and Pt atoms, and the electron redistribution occurs among the energy range from −6 eV to −5 eV. This results in a shift to lower energies of the Pt 5d states, compared with that of the Pt–TiN system before H adsorption. Meanwhile, as shown in Fig. 4b, for the electron transfer between the Pt–H complex and the TiN substrate, there is a significant electron accumulation between Pt and Ti atoms, which is similar to the situation of the Pt–TiN system before H adsorption.[4]

Next, to afford a general understanding and to mimic the effect of electrolytes (*e.g.* H^+ and OH^-) in the fuel cell environment,[27,28] we study the co-adsorption of H and OH with the CO molecule on Pt–TiN(100). As a first step, we approximate the local pH effects of such electrolyte species on the adsorption properties of CO by varying the local surface coverage of H and OH up to a full monolayer surface coverage (corresponding to 9 H or OH on Pt–TiN(100)).

The adsorption energy of CO for co-adsorption with OH (or H) species on Pt–TiN(100) is shown in Fig. 5. Insets are the top views of the atomic structures. As a whole, the adsorption

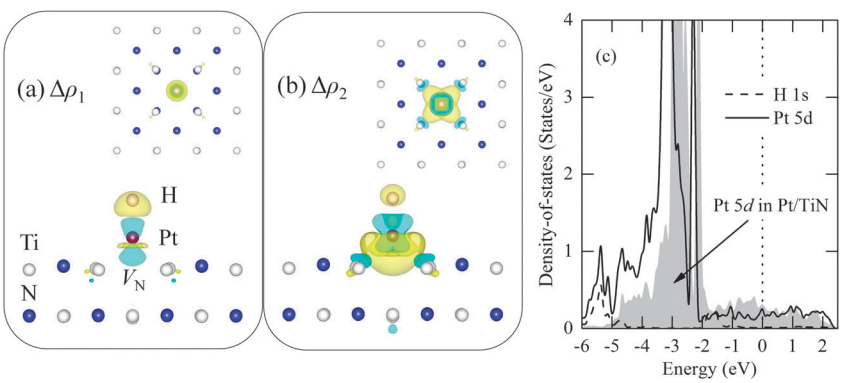

Fig. 4 Side view of electron charge density differences of (a) $\Delta\rho_1$ (*cf.* eqn (4)) and (b) $\Delta\rho_2$ (*cf.* eqn (5)) for H adsorbed on the Pt–TiN system, where the inset shows the corresponding top-view. Charge accumulation and depletion are represented by the yellow and light blue regions, respectively. The isosurface levels are ±0.005 e Bohr^{-3}. (c) The partial density-of-states for H adsorbed on Pt–TiN system. The PDOS for Pt 5d states in Pt–TiN without H represented by the shaded curved are given for comparison. The Fermi energy is indicated by the vertical dotted line at 0 eV.

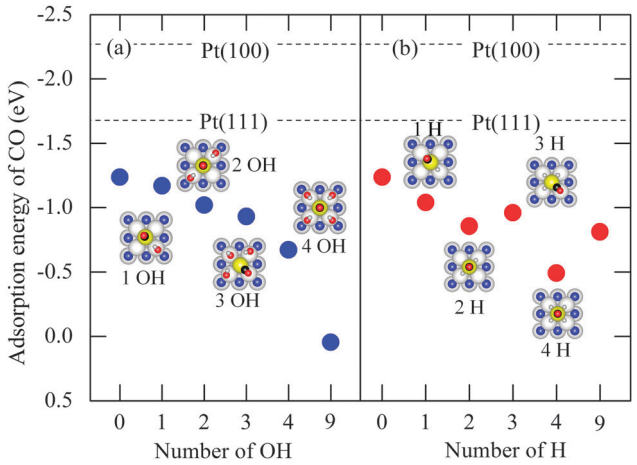

Fig. 5 The adsorption energy (shaded circle) of CO as function of the number of co-adsorbed (a) OH and (b) H groups. Insets are top views of the optimized atomic structures. The horizontal dashed lines indicate the average adsorption energy of the CO molecule on Pt(100) and Pt(111) in the most favorable site. For the situation with 9 OH (or H), the species adsorbed on each T_{Ti} site in the $p(3 \times 3)$ unit cell.

energy of CO increases (becomes less favorable) with increasing number of OH (or H), namely, OH (or H) weakens the adsorption energy of CO. For co-adsorption of CO and OH, when the number of OH increases from 0 to 4, the adsorption energy of CO increases from −1.27 eV to −0.71 eV, a variation of 0.56 eV. OH can be the oxidant for the oxidation of CO. However, when CO binds to the Pt atom and OH binds to the Ti atom, the distance between the carbon monoxide carbon atom of CO and the oxygen atom of OH is too large for the formation of a COOH species. Furthermore, we calculated the adsorption energy for CO on the T_{Pt} site and OH occupying all the T_{Ti} sites in Pt–TiN system. The adsorption energy of CO is just 0.01 eV, which means that it cannot adsorb on the Pt–TiN system. In the situation of co-adsorption with OH, the bond length of C–O is 1.147 Å, which is almost same as free CO of 1.144 Å. This result implies that the CO poisoning would not occur for the Pt–TiN system in OH alkaline environment. We also considered the average adsorption energy of OH on Pt–TiN without CO. The average adsorption energies exhibit only a small variation of about 0.1 eV when the number of OH increases.

For co-adsorption of CO and H, although the adsorption energy of CO decreases slightly (CO becomes more stable) when the number of H increases from 2 to 3, for 4 co-adsorbed H atoms, the adsorption energy of CO increases from −1.27 eV to −0.53 eV, a variation of 0.74 eV. This represents a greater weakening effect compared to OH. This can be understood by combining structures of single H atom adsorption and co-adsorption of H and CO. As mentioned above, a single H atom is unstable on the T_{Ti} site. When H atoms co-adsorb with CO, the initial position of H and CO are T_{Ti} and T_{Pt} site. However, the final optimized structures are H and CO co-adsorbed on Pt atom. It results in the greater weakening effect for CO adsorption.

Overall, compared with CO adsorbed on Pt(100) and (111) surfaces, the adsorption energy of CO on the Pt–TiN surface is weaker. Especially, co-adsorption with H or OH species weakens the adsorption energy of CO. Therefore, Pt–TiN appears more effective than the Pt(111) surface in relation to CO poisoning.

Conclusion

In summary, from the first-principles calculations based on density-functional theory, the adsorption of several molecular species – namely CO_2, CO, O_2, H_2, OH, O, and H, on the Pt–TiN system, as well as the co-adsorption of CO with H or OH, were performed and systemically investigated. We find that the molecular adsorbates CO_2, CO and H bind preferentially to the T_{Pt} site, whilst other molecular absorbates like OH and O prefer the T_{Ti} site. We also find that surface functional groups (*e.g.* OH or H) in the presence of the CO adsorbate drastically weaken the CO adsorption energy on the Pt–TiN(100) surface. On the basis of these findings, we propose that the acid and base conditions in PEM FCs could well provide a possible way to minimize CO poisoning on these surface-functionalized Pt–TiN surfaces.

Acknowledgements

The authors gratefully acknowledge support through a financial award provided by the Asian Office of Aerospace Research and Development (AOARD, Award No. FA2386-12-1-4017), the Australian Research Council (ARC), and partial support by the National Research Foundation of Korea (NRF Grant no. 2011-0013201). Computational resources have been provided by the KISTI supercomputing center (KSC-2012-C2-28, KSC-2013-C2-022), and the Australian National Computational Infrastructure (NCI). RQZ acknowledges the Second Stage of Brain Korea 21 Project (Division of Humantronics Information Materials) for funding.

References

1 D. Ham and J. Lee, *Energies*, 2009, **2**, 873–899.
2 D. Anne-Claire, *Prog. Mater. Sci.*, 2011, **56**, 289–327.
3 H. A. Gasteiger, S. S. Kocha, B. Sompalli and F. T. Wagner, *Appl. Catal., B*, 2005, **56**, 9–35.
4 R. Zhang, T. Lee, B.-D. Yu, C. Stampfl and A. Soon, *Phys. Chem. Chem. Phys.*, 2012, **14**, 16552–16557.
5 R. Ohnishi, M. Katayama, D. Cha, K. Takanabe, J. Kubota and K. Domen, *J. Electrochem. Soc.*, 2013, **160**, F501–F506; R. Ohnishi, K. Takanabe, M. Katayama, J. Kubota and K. Domen, *J. Phys. Chem. C*, 2013, **117**, 496–502; S. Isogai, R. Ohnishi, M. Katayama, J. Kubota, D. Y. Kim, S. Noda, D. Cha, K. Takanabe and K. Domen, *Chem.–Asian J.*, 2012, **7**, 286–289.
6 S. Sun, G. Zhang, N. Gauquelin, N. Chen, J. Zhou, S. Yang, W. Chen, X. Meng, D. Geng, M. N. Banis, R. Li, S. Ye, S. Knights, G. A. Botton, T.-K. Sham and X. Sun, *Sci. Rep.*, 2013, **3**, 1775.
7 Y. Tang, Z. Yang and X. Dai, *J. Nanopart. Res.*, 2012, **14**, 1–11.
8 M. Oana, R. Hoffmann, H. D. Abruña and F. J. DiSalvo, *Surf. Sci.*, 2005, **574**, 1–16.

9 N. Kapur, B. Shan, J. Hyun, L. Wang, S. Yang, J. B. Nicholas and K. Cho, *Mol. Simul.*, 2011, **37**, 648–658.

10 P. C. Jennings, B. G. Pollet and R. L. Johnston, *Phys. Chem. Chem. Phys.*, 2012, **14**, 3134–3139.

11 P. Rodriguez, Y. Kwon and M. T. M. Koper, *Nat. Chem.*, 2012, **4**, 177–182.

12 K. Kershen, H. Celio, I. Lee and J. M. White, *Langmuir*, 2001, **17**, 323–328.

13 T. Zhang, Z.-P. Liu, S. M. Driver, S. J. Pratt, S. J. Jenkins and D. A. King, *Phys. Rev. Lett.*, 2005, **95**, 266102.

14 P. Mohapatra, J. Moma, K. M. Parida, W. A. Jordaan and M. S. Scurrell, *Chem. Commun.*, 2007, 1044–1046.

15 L.-Y. Gan and Y.-J. Zhao, *J. Chem. Phys.*, 2010, **133**, 094703.

16 P. Rodríguez, A. A. Koverga and M. T. M. Koper, *Angew. Chem., Int. Ed.*, 2010, **49**, 1241–1243.

17 L.-Y. Gan, R.-Y. Tian, X.-B. Yang, S.-L. Peng and Y.-J. Zhao, *Phys. Chem. Chem. Phys.*, 2011, **13**, 14466–14475.

18 M. M. O. Thotiyl and S. Sampath, *Electrochim. Acta*, 2011, **56**, 3549–3554.

19 G. Kresse and J. Hafner, *Phys. Rev. B: Condens. Matter Mater. Phys.*, 1993, **47**, 558.

20 G. Kresse and J. Furthmüller, *Phys. Rev. B: Condens. Matter Mater. Phys.*, 1996, **54**, 11169.

21 G. Kresse and D. Joubert, *Phys. Rev. B: Condens. Matter Mater. Phys.*, 1999, **59**, 1758–1775.

22 J. P. Perdew, K. Burke and M. Ernzerhof, *Phys. Rev. Lett.*, 1996, **77**, 3865.

23 T.-H. Lee, B. Delley, C. Stampfl and A. Soon, *Nanoscale*, 2012, **4**, 5183–5188.

24 G. Makov and M. C. Payne, *Phys. Rev. B: Condens. Matter Mater. Phys.*, 1995, **51**, 4014.

25 W. Liu, Y. F. Zhu, J. S. Lian and Q. Jiang, *J. Phys. Chem. C*, 2006, **111**, 1005–1009.

26 H. Steininger, S. Lehwald and H. Ibach, *Surf. Sci.*, 1982, **123**, 264–282.

27 J. Rossmeisl, K. Chan, R. Ahmed, V. Tripkovic and M. E. Bjorketun, *Phys. Chem. Chem. Phys.*, 2013, **15**, 10321–10325.

28 J. Rossmeisl, E. Skúlason, M. E. Björketun, V. Tripkovic and J. K. Nørskov, *Chem. Phys. Lett.*, 2008, **466**, 68–71.

29 Section of Spectroscopic Constants of Diatomic Molecules, in *CRC Handbook of Chemistry and Physics*, Taylor and Francis, Boca Raton, FL, 1987, p. 103.

